

Neutral Higgs boson pair production at the linear collider in the noncommutative standard modelPrasanta Kumar Das,^{*} Abhishodh Prakash,[†] and Anupam Mitra[‡]*Birla Institute of Technology and Science-Pilani, K.K. Birla Goa Campus, NH-17B, Zuarinagar, Goa-403726, India*

(Received 19 September 2010; published 3 March 2011)

We study the Higgs boson pair production at the linear collider in the noncommutative extension of the standard model using the Seiberg-Witten map of this to the first order of the noncommutative parameter $\Theta_{\mu\nu}$. Unlike the standard model (where the process is forbidden) here the Higgs boson pair directly interacts with the photon. We find that the pair production cross section can be quite significant for the noncommutative scale Λ lying in the range 0.5 TeV to 1.0 TeV. Using the experimental (LEP 2, Tevatron, and global electroweak fit) bound on the Higgs mass, we obtain $626 \text{ GeV} \leq \Lambda \leq 974 \text{ GeV}$.

DOI: 10.1103/PhysRevD.83.056002

PACS numbers: 11.10.Nx, 14.80.Ec

I. INTRODUCTION

In spite of its enormous experimental success the standard model (SM) of particle physics still awaits the discovery of the Higgs boson. After the Large Electron Positron (LEP) collider has set a lower limit of about 114.4 GeV on its mass [1], the responsibility of finding the Higgs boson now rests mostly on the Large Hadron Collider (LHC) at CERN which has started its operation. At the same time, puzzles like the naturalness problem make a strong case for physics beyond the standard model (SM), just around or above the mass scale where the Higgs boson is expected to be found out. It is therefore of supreme interest to see if the collider signals of the Higgs boson contain some imprints of new physics. This necessitates detailed quantitative exploration of a variety of phenomena linked to the production and decays of the Higgs boson.

In this paper, we study the pair production of the Higgs boson in the intermediate and heavy mass range at the linear collider (LC) as a possible channel for uncovering new physics effects. In particular, we show that although the pair production is forbidden in the SM with the space-time background being commutative (we will call this CSM in abbreviation) it receives a large contribution in the noncommutative (NC) extension of the SM (which will be dubbed NCSM).

As has been mentioned above, the large hierarchy between the electroweak scale M_W and the Planck scale M_{Pl} is somewhat puzzling. Though theories like supersymmetry and technicolor, each with its own phenomenological implications and constraints, have been proposed as a resolution of this problem, the idea of extra spatial dimensions, with the scale of gravity being as low as TeV, has drawn a lot of interest among the physics community recently [2]. In some brane-world models [3] where this TeV scale gravity is realized, one can principally expect to

see some stringy effects in the upcoming TeV colliders and in addition the signature of space-time noncommutativity. Interest in the noncommutative field theory arose from the pioneering work by Snyder [4] and has been revived recently due to developments connected to string theories in which the noncommutativity of space-time is an important characteristic of D-brane dynamics at a low energy limit [5–7]. Although Douglas *et al.* [6] in their pioneering work have shown that noncommutative field theory is a well-defined quantum field theory, the question that remains is whether the string theory prediction and the noncommutative effect can be seen at the energy scale attainable in present or near future experiments instead of the four-dimensional Planck scale M_{Pl} . A notable work by Witten [8] suggests that one can see some stringy effects by lowering the threshold value of commutativity to TeV, a scale which is not so far from present or future collider scale.

What is the space-time noncommutativity? It means space and time no longer commute with each other and one cannot measure the space and time coordinates simultaneously with the same accuracy. Writing the space-time coordinates as operators, we find

$$[\hat{X}_\mu, \hat{X}_\nu] = i\Theta_{\mu\nu}, \quad (1)$$

where the matrix $\Theta_{\mu\nu}$ is real and antisymmetric. The noncommutative parameter $\Theta_{\mu\nu}$ has dimension of area and reflects the extent to which the space-time coordinates are noncommutative, i.e. fuzzy. Furthermore, introducing a NC scale Λ , we rewrite Eq. (1) as

$$[\hat{X}_\mu, \hat{X}_\nu] = \frac{i}{\Lambda^2} c_{\mu\nu}, \quad (2)$$

where $\Theta_{\mu\nu}(= c_{\mu\nu}/\Lambda)$ and $c_{\mu\nu}$ has the same properties as $\Theta_{\mu\nu}$. To study an ordinary field theory in such a noncommutative fuzzy space, one replaces all ordinary products among the field variables with Moyal-Weyl (MW) [9] \star products defined by

$$(f \star g)(x) = \exp\left(\frac{1}{2}\Theta_{\mu\nu}\partial_{x^\mu}\partial_{y^\nu}\right)f(x)g(y)|_{y=x}. \quad (3)$$

^{*}Corresponding author.

pdas@bits-goia.ac.in, pdasMaparna@gmail.com

[†]abhishodh@gmail.com[‡]anupam.mitra@gmail.com

Using this we can get the NC QED Lagrangian as

$$\begin{aligned} \mathcal{L} = & \frac{1}{2} i(\bar{\psi} \star \gamma^\mu D_\mu \psi - (D_\mu \bar{\psi}) \star \gamma^\mu \psi) \\ & - m \bar{\psi} \star \psi - \frac{1}{4} F_{\mu\nu} \star F^{\mu\nu}, \end{aligned} \quad (4)$$

which is invariant under the following transformations:

$$\psi(x, \Theta) \rightarrow \psi'(x, \Theta) = U \star \psi(x, \Theta), \quad (5)$$

$$\begin{aligned} A_\mu(x, \Theta) & \rightarrow A'_\mu(x, \Theta) \\ & = U \star A_\mu(x, \Theta) \star U^{-1} + \frac{i}{e} U \star \partial_\mu U^{-1}, \end{aligned} \quad (6)$$

where $U = (e^{i\Lambda})_\star$. In the NC QED Lagrangian [Eq. (4)] $D_\mu \psi = \partial_\mu \psi - ieA_\mu \star \psi$, $(D_\mu \bar{\psi}) = \partial_\mu \bar{\psi} + ie\bar{\psi} \star A_\mu$, $F_{\mu\nu} = \partial_\mu A_\nu - \partial_\nu A_\mu - ie(A_\mu \star A_\nu - A_\nu \star A_\mu)$.

The alternative is the Seiberg-Witten (SW)[5–7,10] approach in which both the gauge parameter Λ and the gauge field A^μ are expanded as

$$\begin{aligned} \Lambda_\alpha(x, \Theta) = & \alpha(x) + \Theta^{\mu\nu} \Lambda_{\mu\nu}^{(1)}(x; \alpha) \\ & + \Theta^{\mu\nu} \Theta^{\eta\sigma} \Lambda_{\mu\nu\eta\sigma}^{(2)}(x; \alpha) + \dots, \end{aligned} \quad (7)$$

$$\begin{aligned} A_\rho(x, \Theta) = & A_\rho(x) + \Theta^{\mu\nu} A_{\mu\nu\rho}^{(1)}(x) \\ & + \Theta^{\mu\nu} \Theta^{\eta\sigma} A_{\mu\nu\eta\sigma\rho}^{(2)}(x) + \dots, \end{aligned} \quad (8)$$

and when the field theory is expanded in terms of this power series [Eq. (7)] one ends up with an infinite tower of higher dimensional operators which renders the theory nonrenormalizable. However, the advantage is that this construction can be applied to any gauge theory with arbitrary matter representation. In the MW approach the group closure property is only found to hold for the $U(N)$ gauge theories and the matter content is found to be in the (anti)fundamental and adjoint representations. Using the SW map, Calmet *et al.* [11] first constructed a model with noncommutative gauge invariance which was close to the usual commuting standard model and is known as the *minimal* noncommutative standard model (mNCSM), in which they listed several Feynman rules comprising NC interaction. Intense phenomenological searches [12] have been made to unravel several interesting features of this mNCSM. Hewett *et al.* explored several processes

e.g. $e^+e^- \rightarrow e^+e^-$; Bhabha, $e^-e^- \rightarrow e^-e^-$; Möller, $e^- \gamma \rightarrow e^- \gamma$, $e^+e^- \rightarrow \gamma\gamma$ (pair annihilation), $\gamma\gamma \rightarrow e^+e^-$, and $\gamma\gamma \rightarrow \gamma\gamma$ in the context of NC QED. Recently, in Ref. [13] one of us has investigated the impact of Z and photon exchange in the Bhabha and the Möller scattering and three of us have reported the impact of space-time noncommutativity in the muon pair production at the LC [14]. Now in a generic NC QED the triple photon vertex arises to order $\mathcal{O}(\Theta)$, which however is absent in this mNCSM. Another formulation of the NCSM came to the forefront through the pioneering work by Melić *et al.* [15] where such a triple neutral gauge boson coupling [16] appears naturally in the gauge sector. We will call this the *nonminimal version* of NCSM or simply nmNCSM. We work in the nmNCSM scenario and use the Feynman rules for interactions given in Melić *et al.* [15].

In Sec. II we analyze the Higgs pair production $e^+e^- \rightarrow \gamma, Z \rightarrow HH$ in the nmNCSM. We describe the pair production cross section, angular distribution, and the prospects of TeV scale noncommutative geometry in Sec. III. Numerical analysis is presented in detail in this section. Finally, we conclude in Sec. IV.

II. HIGGS PAIR PRODUCTION AT THE FUTURE LINEAR COLLIDER

Since there is no direct interaction of a photon (or a Z boson) with the Higgs pair, the pair production of the Higgs boson through e^+e^- annihilation in the standard model is forbidden. So the finding of any nonzero event rate of the Higgs pair production may be interpreted as the signature of new physics. Supersymmetry, brane-world gravity, and noncommutative geometry are the possible potential candidates (see [17] and references therein). Here we explore the potential feasibility of the nmNCSM. In this model the Higgs pair production proceeds via the s channel exchange of photon and Z boson, i.e. $e^+e^- \rightarrow \gamma, Z \rightarrow HH$. The corresponding Feynman diagrams are shown in Fig. 1. The scattering amplitude [using Feynman rules to order Θ (shown in Appendix A)] can be written as

$$i\mathcal{A} = i(\mathcal{A}_\gamma + \mathcal{A}_Z), \quad (9)$$

where A_γ and A_Z can be calculated as

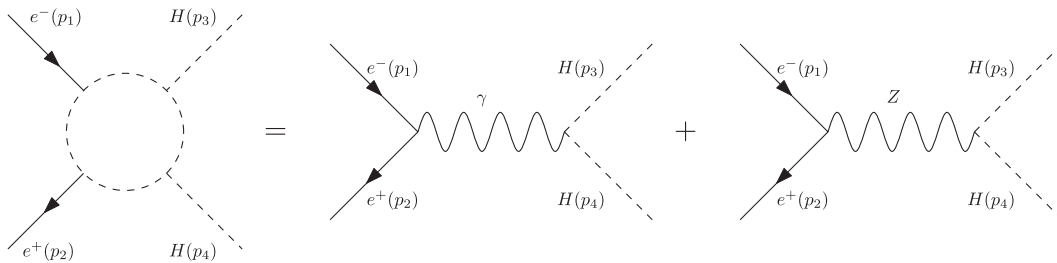


FIG. 1. Feynman diagrams for $e^+e^- \rightarrow \gamma, Z \rightarrow HH$ in the nmNCSM.

$$i\mathcal{A}_\gamma = \frac{\pi\alpha M_H^2}{s} [\bar{v}(p_2)\gamma_\mu u(p_1)] \times (k\Theta)^\mu \left[1 + \frac{i}{2}(p_2\Theta p_1) \right], \quad (10)$$

$$i\mathcal{A}_Z = \frac{\pi\alpha M_H^2}{\sin^2(2\theta_W)(s - m_Z^2 + i\Gamma_Z m_Z)} \times [\bar{v}(p_2)\gamma_\mu (4\sin^2(\theta_W) - 1 + \gamma^5)u(p_1)](k\Theta)^\mu \times \left[1 + \frac{i}{2}(p_2\Theta p_1) \right], \quad (11)$$

where $s = (p_1 + p_2)^2$, $k = (p_1 + p_2) = (p_3 + p_4)$, $\alpha = e^2/4\pi$, and θ_W is the Weinberg angle. M_H is the Higgs mass and m_Z and Γ_Z are the mass and decay width of the Z boson. The spin averaged squared-amplitude is given by

$$|\overline{\mathcal{A}}|^2 = |\overline{\mathcal{A}_\gamma}|^2 + |\overline{\mathcal{A}_Z}|^2 + 2\text{Re}(\overline{\mathcal{A}_\gamma}\overline{\mathcal{A}_Z}^\dagger). \quad (12)$$

Several terms of Eq. (12) are given in Appendix C. The differential cross section can be written as

$$\frac{d\sigma}{d\Omega} = \frac{1}{64\pi^2 s} \frac{\lambda^{1/2}(s, M_H^2, M_H^2)}{s} |\overline{\mathcal{A}}|^2, \quad (13)$$

where $\sigma = \sigma(\sqrt{s}, \Lambda, \theta, \phi)$ and λ is the Kallen function defined as $\lambda(x, y, z) = x^2 + y^2 + z^2 - 2xy - 2yz - 2zx$. From Eq. (13) we can obtain σ , $d\sigma/d\cos\theta$, and $d\sigma/d\phi$ as

$$\sigma = \int_{-1}^1 d(\cos\theta) \int_0^{2\pi} d\phi \frac{d\sigma}{d\Omega}, \quad (14)$$

$$\frac{d\sigma}{d\cos\theta} = \int_0^{2\pi} d\phi \frac{d\sigma}{d\Omega}, \quad (15)$$

$$\frac{d\sigma}{d\phi} = \int_{-1}^1 d(\cos\theta) \frac{d\sigma}{d\Omega}. \quad (16)$$

III. NUMERICAL ANALYSIS

In this section, we analyze the total cross section and angular distributions of the cross section of the neutral Higgs pair production. Before this, let us make some general remarks regarding the observation of noncommutative effects. Because we assume $c_{\mu\nu} = (c_{0i}, c_{ij}) = (\xi_i, \epsilon_{ijk}\chi^k)$, where $\xi_i = (\vec{E})_i$ and $\chi_k = (\vec{B})_k$ are constant vectors in a frame that is stationary with respect to fixed stars, the vectors $(\vec{E})_i$ and $(\vec{B})_k$ point in fixed directions which are the same in all frames of reference. However, as the Earth rotates around its axis and revolves around the Sun, the direction of \vec{E} and \vec{B} will change continuously with time dependence, which is a function of the coordinates of the laboratory. The observables that are measured will thus show a characteristic time dependence. It is important to be able to measure this time dependence to verify such noncommutative theories. In our analysis, we have assumed the vectors $\vec{E} = \frac{1}{\sqrt{3}}(\hat{i} + \hat{j} + \hat{k})$ and $\vec{B} = \frac{1}{\sqrt{3}}(\hat{i} + \hat{j} + \hat{k})$, i.e. they behave like constant vectors. This can be true only at some instant of time at most.

A. Pair production cross section in the nmNCSM

In Fig. 2 we have plotted the pair production cross section $\sigma(e^-e^+ \rightarrow \gamma, Z \rightarrow HH)$ as a function of the Higgs mass m_H (GeV). The machine energy $E_{\text{com}} (= \sqrt{s})$ is fixed at 500 GeV and 1000 GeV, respectively. The curves from top to bottom in each figure correspond to $\Lambda = 500, 600, 700, 800, 900,$ and 1000 GeV, respectively. The cross section attains its maximum value at $m_H = 220$ GeV and 451 GeV, corresponding to the machine energy $E_{\text{com}} = 500$ GeV and 1000 GeV, respectively. Assuming the integrated luminosity of the future LC as $\mathcal{L} = 500 \text{ fb}^{-1}$, we predict the number of events of Higgs pair production in

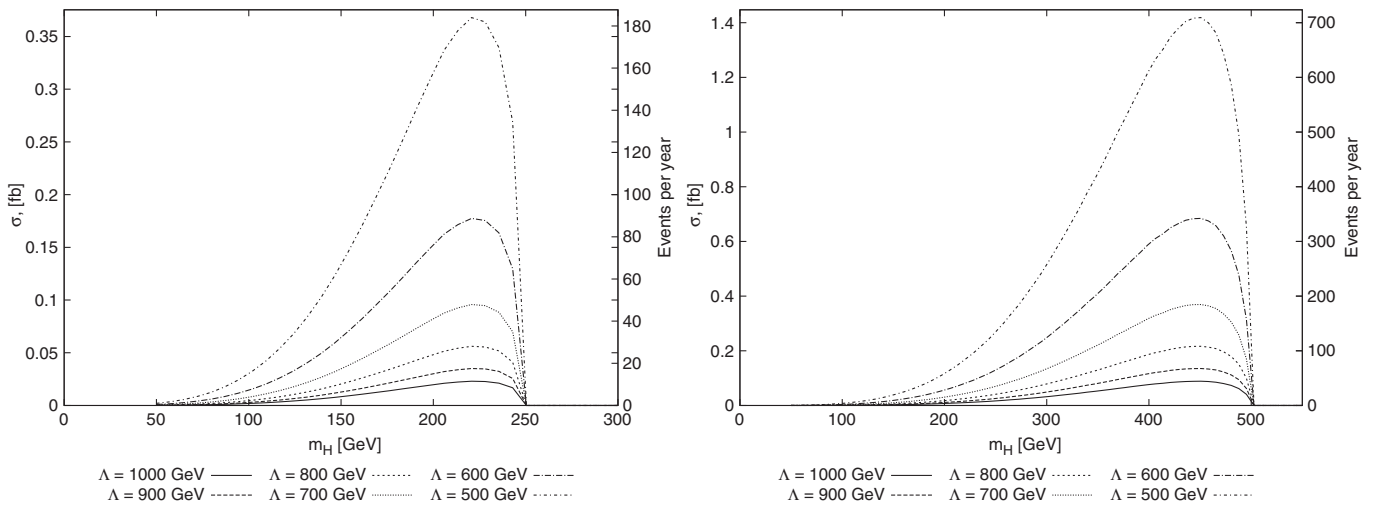


FIG. 2. The cross section $\sigma(e^-e^+ \rightarrow Z \rightarrow HH)$ (fb) as a function of the Higgs mass m_H (GeV) is shown. In the left (right) panel, center-of-mass energy is fixed at $\sqrt{s} = 500(1000)$ GeV. In a given figure, from the top to bottom Λ increases from 500 GeV to 1000 GeV in steps of 100 GeV.

TABLE I. The maximum number of events (yr^{-1}) as a function of Λ (GeV) is shown. The peaks are at $m_H = 220$ GeV and 451 GeV corresponding to the machine energy $E_{\text{com}} = 500$ GeV and 1000 GeV, respectively. The integrated luminosity for the LC is assumed to be $\mathcal{L} = 500 \text{ fb}^{-1}$.

\sqrt{s}	Λ	$\sigma(\text{fb})$	$\mathcal{L}(\text{fb}^{-1})$	$N \text{ yr}^{-1}$
500	500	0.3679	500	184
	600	0.1774	500	89
	700	0.0958	500	48
	800	0.0561	500	28
	900	0.0351	500	18
	1000	0.0229	500	11
1000	500	1.4188	500	709
	600	0.6749	500	337
	700	0.3693	500	185
	800	0.2165	500	108
	900	0.1351	500	67
	1000	0.0887	500	44

the nmNCSM. In Table I, the number of events N (yr^{-1}) as a function of Λ corresponding to the machine energy $E_{\text{com}} = 500$ GeV and 1000 GeV are shown. Interestingly with the increase in Λ from 500 GeV to 1000 GeV, the number of events (NC signals) $N(\text{yr}^{-1})$ decreases from 184 (709) per year to 11 (44) per year. So a maximum of 184 and 709 events (NC signal) per year is expected to be observed at the future LC.

These are to be compared with the zero event prediction in the CSM.

B. Constraining Λ using the experimental bound on Higgs mass m_H

In the earlier subsection we found that the Higgs pair production cross section is maximum at $m_H = 220$ GeV and 451 GeV corresponding to the machine energy $\sqrt{s} = 500$ GeV and 1000 GeV and for the NC scale $\Lambda = 500$ GeV. In Fig. 3 we make a contour plot in $m_H - \Lambda$ plane corresponding to the event rate $N(\text{yr}^{-1})$. The integrated luminosity \mathcal{L} is assumed to be 500 fb^{-1} . The results are presented below:

Scenario I: $11 \leq N \leq 184$ and the center-of-mass energy $\sqrt{s} = 500$ GeV,

Scenario II: $44 \leq N \leq 709$ and the center-of-mass energy $\sqrt{s} = 1000$ GeV.

The following observations are in order:

- (1) The direct search of Higgs boson at LEP 2 gives a lower bound on Higgs mass m_H as 114.4 GeV. Incorporating this in Fig. (3), one finds: (i) $\Lambda > 626$ GeV in scenario I and (ii) $\Lambda > 313$ GeV in scenario II.
- (2) The combined CDF and D0 Collaboration data at Tevatron, Fermilab excludes m_H lying between $158 \text{ GeV} \leq m_H \leq 175 \text{ GeV}$. Translating this in Fig. 3, one finds $\Lambda \leq 828$ GeV and $\Lambda \geq 892$ GeV

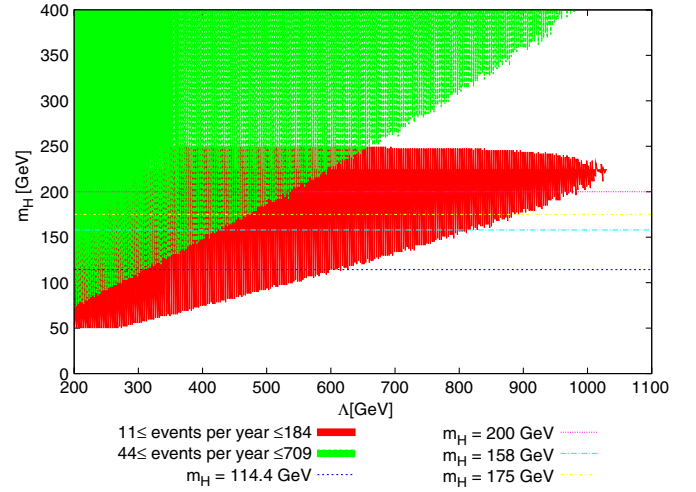


FIG. 3 (color online). The contour plot in the $m_H - \Lambda$ plane obtained by setting $11 \leq N(\text{yr}^{-1}) \leq 184$ (lower) and $44 \leq N(\text{yr}^{-1}) \leq 709$ (upper) corresponding to $\sqrt{s} = 500$ GeV and 1000 GeV, respectively. The lowermost and uppermost horizontal lines correspond to the lower and upper bound on the Higgs mass m_H which follows from the LEP 2 direct search and the global electroweak fit. The combined CDF and D0 data at Tevatron excludes $158 \text{ GeV} \leq m_H \leq 175 \text{ GeV}$.

in scenario I and $\Lambda \leq 428$ GeV and $\Lambda \geq 475$ GeV in scenario II.

- (3) The global electroweak fit suggests $m_H \leq 200$ GeV. Translating this in Fig. (3), one finds $\Lambda \leq 974$ GeV in scenario I and $\Lambda \leq 537$ GeV in scenario II.

Altogether, the LEP 2, Tevatron, and global electroweak fit to m_H imposes the following bound on Λ :

- (1) $626 \text{ GeV} \leq \Lambda \leq 828 \text{ GeV}$ and $892 \text{ GeV} \leq \Lambda \leq 974 \text{ GeV}$ in scenario I.
- (2) $313 \text{ GeV} \leq \Lambda \leq 428 \text{ GeV}$ and $475 \text{ GeV} \leq \Lambda \leq 537 \text{ GeV}$ in scenario II.

IV. CONCLUSION

The TeV scale space-time noncommutativity recently has drawn a lot of attention among the physics community. Here we have investigated the effect of space-time noncommutativity on the pair production Higgs boson through $e^+ - e^-$ collision in the nmNCSM. The process is forbidden in the CSM. The cross section $\sigma(e^+e^- \rightarrow \gamma, Z \rightarrow HH)$ is found to be peaked at $m_H = 220$ and 451 GeV corresponding to the machine energy $E_{\text{com}} (= \sqrt{s}) = 500$ GeV and 1000 GeV, respectively. Accordingly, the maximum event rate is found to be $184(\text{yr}^{-1})$ and $709(\text{yr}^{-1})$ where we have assumed the integrated luminosity of about 500 fb^{-1} for the LC. We obtain a contour plot in the plane of $m_H - \Lambda$ corresponding to the event rate $11 \leq N(\text{yr}^{-1}) \leq 184$ and $44 \leq N(\text{yr}^{-1}) \leq 709$. The direct searches of Higgs boson at LEP 2, Tevatron at Fermilab, and global electroweak fit to m_H impose some bounds on

m_H . Incorporating these on the contour plot, we obtain the following bounds on Λ : (i) $626 \text{ GeV} \leq \Lambda \leq 828 \text{ GeV}$ and $892 \text{ GeV} \leq \Lambda \leq 974 \text{ GeV}$ in scenario I and (ii) $313 \text{ GeV} \leq \Lambda \leq 428 \text{ GeV}$ and $475 \text{ GeV} \leq \Lambda \leq 537 \text{ GeV}$ in scenario II. Finally, we found that the azimuthal distribution ($d\sigma/d\phi$) and the polar distribution $d\sigma/d\cos\theta$ are insensitive to the angles ϕ and $\cos\theta$, irrespective of the machine energy and the NC scale Λ .

So, the noncommutative geometry is found to be quite rich in terms of its phenomenological implications and it is worthwhile to explore several other processes which might be potentially relevant for linear collider experiments.

ACKNOWLEDGMENTS

The work of P. K. Das is supported by the DST Fast Track Young Scientist Project No. SR/FTP/PS-11/2006. P. K. Das would also like to thank Dr. Chandradew Sharma and Dr. Tarun Kumar Jha of the physics department of BITS-Pilani, K. K. Birla Goa campus, for several useful discussions.

APPENDIX A: FEYNMAN RULES TO ORDER $O(\Theta)$

The Feynman rule for the $f(p_{\text{in}}) - f(p_{\text{out}}) - \gamma(k)$ vertex, (where f represents a fermion), to $O(\Theta)$ can be written as [15]

$$\begin{aligned} ieQ_f \left[\gamma_\mu - \frac{i}{2} k^\nu (\Theta_{\mu\nu\rho} p_{\text{in}}^\rho - \Theta_{\mu\nu} m_f) \right] \\ = ieQ_f \gamma_\mu + \frac{1}{2} eQ_f [(p_{\text{out}} \Theta p_{\text{in}}) \gamma_\mu \\ - (p_{\text{put}} \Theta)_\mu (p_{\text{in}} - m_f) - (p_{\text{out}} - m_f) (\Theta p_{\text{in}})_\mu]. \end{aligned} \quad (\text{A1})$$

and for the vertex $f(p_{\text{in}}) - f(p_{\text{out}}) - Z(k)$ is

$$\begin{aligned} \frac{e}{\sin 2\theta_W} [i\gamma_\mu \Gamma_A^-] + \frac{e}{2 \sin 2\theta_W} [(p_{\text{out}} \Theta p_{\text{in}}) \gamma_\mu \Gamma_A^- \\ - (p_{\text{put}} \Theta)_\mu \Gamma_A^+ (p_{\text{in}} - m_f) - (p_{\text{out}} - m_f) \Gamma_A^- (\Theta p_{\text{in}})_\mu]. \end{aligned} \quad (\text{A2})$$

The momentum conservation reads as $p_{\text{in}} + k = p_{\text{out}}$. Similarly, the Feynman rule for the interaction vertex $H(p) - H(p') - Z(k)$ is

$$\frac{gM_H^2(k\Theta)_\mu}{4 \cos\theta_W} \quad (\text{A3})$$

and for the vertex $H(p) - H(p') - \gamma(k)$ is

$$\frac{eM_H^2(k\Theta)_\mu}{4}. \quad (\text{A4})$$

In the above expressions, $(k\Theta)_\mu = k_{\mu\nu} \Theta^\nu$, $\Gamma_A^\pm = (c_V^e \pm c_A^e \gamma_5)$. Also $p_{\text{out}} \Theta p_{\text{in}} = p_{\text{out}}^\mu \Theta_{\mu\nu} p_{\text{in}}^\nu = -p_{\text{in}} \Theta p_{\text{out}}$.

APPENDIX B: MOMENTUM PRESCRIPTIONS AND DOT PRODUCTS

The four momenta of the particles [involved in scattering $e^-(p_1)e^+(p_2) \rightarrow H(p_3)H(p_4)$] in the center-of-mass frame are specified as

$$p_1 = \left(\frac{\sqrt{s}}{2}, 0, 0, \frac{\sqrt{s}}{2} \right), \quad (\text{B1})$$

$$p_2 = \left(\frac{\sqrt{s}}{2}, 0, 0, -\frac{\sqrt{s}}{2} \right), \quad (\text{B2})$$

$$p_3 = \left(\frac{\sqrt{s}}{2}, k' \sin\theta \cos\phi, k' \sin\theta \sin\phi, k' \cos\theta \right), \quad (\text{B3})$$

$$p_4 = \left(\frac{\sqrt{s}}{2}, -k' \sin\theta \cos\phi, -k' \sin\theta \sin\phi, -k' \cos\theta \right),$$

$$k' = \frac{\sqrt{s}}{2} \sqrt{1 - \frac{4M_H^2}{s}}. \quad (\text{B4})$$

Here θ is the scattering angle made by the 3-momentum vector p_3 with the positive Z axis and ϕ is the azimuthal angle. We note that the antisymmetric $\Theta_{\mu\nu}$ has six independent components corresponding to $c_{\mu\nu} = (c_{0i}, c_{ij})$ with $i, j = 1, 2, 3$. Assuming all of them are nonvanishing they can be written in the form

$$c_{0i} = \frac{\xi_i}{\Lambda^2}, \quad (\text{B5})$$

$$c_{ij} = \frac{\epsilon_{ijk} \chi^k}{\Lambda^2}. \quad (\text{B6})$$

The antisymmetric $\Theta_{\mu\nu}$ is analogous to the field tensor $F_{\mu\nu}$, where ξ_i and χ_i are like the components of the electric and magnetic field vectors. Setting $\xi_i = (\vec{E})_i = \frac{1}{\sqrt{3}}$ and $\chi_i = (\vec{B})_i = \frac{1}{\sqrt{3}}$, with $i = 1, 2, 3$, and noting $\chi_i = -\chi^i$, $\xi_i = -\xi^i$, and $\xi_i \xi^j = \frac{1}{3} \delta_i^j$ and $\chi_i \chi^j = \frac{1}{3} \delta_i^j$, we find

$$p_2 \Theta p_1 = \frac{s}{2\sqrt{3}\Lambda^2}, \quad (\text{B7})$$

$$(k\Theta)_0 = 0, \quad (\text{B8})$$

$$(k\Theta)_1 = \frac{\sqrt{s}}{\sqrt{3}\Lambda^2}, \quad (\text{B9})$$

$$(k\Theta)_2 = \frac{\sqrt{s}}{\sqrt{3}\Lambda^2}, \quad (\text{B10})$$

$$(k\Theta)_3 = \frac{\sqrt{s}}{\sqrt{3}\Lambda^2}, \quad (\text{B11})$$

where $k = p_1 + p_2 = p_3 + p_4$ and $p_1 \cdot p_2 = s/2$.

APPENDIX C: SPIN-AVERAGED SQUARED-AMPLITUDE

From Eq. (12) we find

$$\begin{aligned} |\overline{\mathcal{A}}|^2 &= |\overline{\mathcal{A}}_\gamma|^2 + |\overline{\mathcal{A}}_Z|^2 + 2\text{Re}(\overline{\mathcal{A}}_\gamma \overline{\mathcal{A}}_{Z^\dagger}) \\ &= \frac{1}{4} \sum_{\text{spin}} |\mathcal{A}|^2. \end{aligned} \quad (\text{C1})$$

The various components of the above squared-matrix element are found to be

$$|\overline{A}_\gamma|^2 = -\frac{\pi^2 \alpha^2 M_H^4}{s^2} F, \quad (\text{C2})$$

$$|\overline{A}_Z|^2 = -\frac{\pi^2 \alpha^2 M_H^4 [1 + (4\sin^2 \Theta_w - 1)^2]}{\sin^4(2\theta_w) [(s - m_Z^2)^2 + \Gamma_Z^2 M_Z^2]} F, \quad (\text{C3})$$

$$2\text{Re}(\overline{A}_\gamma^\dagger \overline{A}_Z) = \frac{2\pi^2 \alpha^2 M_H^4 (4\sin^2 \Theta_w - 1)(s - m_Z^2)}{\sin^2(2\theta_w) s [(s - m_Z^2)^2 + \Gamma_Z^2 M_Z^2]} F. \quad (\text{C4})$$

The overall factor F is given by

$$F = [2(p_1 \Theta p_2)^2 + (p_1 \cdot p_2)((p_1 + p_2) \Theta \cdot (p_1 + p_2) \Theta)]. \quad (\text{C5})$$

Several dot product terms appearing above are listed in Appendix B. Note that the above expressions from Eqs.(C2)–(C5) are independent of θ and ϕ .

-
- [1] T. Junk (The LEP Higgs Working Group), in Proceedings of the LEP Fest, October 2000 (unpublished).
- [2] N. Arkani-Hamed, S. Dimopoulos, and G. Dvali, *Phys. Lett. B* **429**, 263 (1998).
- [3] N. Arkani-Hamed, S. Dimopoulos, and G. Dvali, *Phys. Lett. B* **429**, 263 (1998); I. Antoniadis, N. Arkani-Hamed, S. Dimopoulos, and G. Dvali, *Phys. Lett. B* **436**, 257 (1998).
- [4] H. S. Snyder, *Phys. Rev.* **72**, 68 (1947).
- [5] A. Connes, M. R. Douglas, and A. Schwarz, *J. High Energy Phys.* **02** (1998) 003.
- [6] M. R. Douglas and C. Hull, *J. High Energy Phys.* **02** (1998) 008.
- [7] N. Seiberg and E. Witten, *J. High Energy Phys.* **09** (1999) 032.
- [8] E. Witten, *Nucl. Phys.* **B471**, 135 (1996); P. Horava and E. Witten, *Nucl. Phys.* **B460**, 506 (1996).
- [9] M. R. Douglas and N. Nekrasov, *Rev. Mod. Phys.* **73**, 977 (2001); I. F. Riad and M. M. Sheikh-Jabbari, *J. High Energy Phys.* **08** (2000) 045; B. Jurco and P. Schupp, *Eur. Phys. J. C* **14**, 367 (2000).
- [10] B. Jurco, P. Schupp, and J. Wess, *Mod. Phys. Lett. A* **16**, 343 (2001).
- [11] X. Calmet, B. Jurco, P. Schupp, J. Wess, and M. Wohlgenannt, *Eur. Phys. J. C* **23**, 363 (2002); *Eur. Phys. J. C* **50**, 113 (2007).
- [12] J. Hewett, F. J. Petriello, and T. G. Rizzo, *Proceedings of the 2001 Snowmass Summer Study*, econf C010630 (2001); J. Hewett *et al.*, *Phys. Rev. D* **64**, 075012 (2001); **66**, 036001 (2002); T. G. Rizzo, *Int. J. Mod. Phys. A* **18**, 2797 (2003); A. Alboteanu, T. Ohl, and R. Ruckl, *Acta Phys. Pol. B* **38**, 3647 (2007).
- [13] P. K. Das *et al.*, *Phys. Rev. D* **77**, 035010 (2008).
- [14] P. Abhishodh. A. Mitra, and P. K. Das, *Phys. Rev. D* **82**, 055020 (2010).
- [15] B. Melić, K. P. Kumericki, J. Trampetic, P. Schupp, and M. Wohlgenannt, *Eur. Phys. J. C* **42**, 499 (2005); P. Schupp and J. Trampetic, *Springer Proc. Phys.* **98**, 219 (2005).
- [16] G. Duplancic, P. Schupp, and J. Trampetic, *Eur. Phys. J. C* **32**, 141 (2003); W. Behr, N. G. Deshpande, G. Duplancic, P. Schupp, J. Trampetic, and J. Wess, *Eur. Phys. J. C* **29**, 441 (2003); P. Aschieri, B. Jurco, P. Schupp, and J. Wess, *Nucl. Phys.* **B651**, 45 (2003).
- [17] P. K. Das and B. Mukhopadhyaya, *arXiv:hep-ph/0303135*.